Reactive Molecular Dynamics Simulation of Solid Nitromethane Impact on (010) Surfaces Induced and Nonimpact Thermal Decomposition

3 **AUTHORS**, INCLUDING:

Feng Guo
Liaocheng Universtiy
**6** PUBLICATIONS   **33** CITATIONS

Reactive Molecular Dynamics Simulation of Solid Nitromethane Impact on (010) Surfaces Induced and Nonimpact Thermal Decomposition

Feng Guo,[†] Xin-lu Cheng,[†] and Hong Zhang*,[‡]

[†]Institute of Atomic and Molecular Physics and [‡]School of Physical Science & Technology, Sichuan University, Chengdu, Sichuan Province, P. R. C.

Ⓢ *Supporting Information*

ABSTRACT: Which is the first step in the decomposition process of nitromethane is a controversial issue, proton dissociation or C–N bond scission. We applied reactive force field (ReaxFF) molecular dynamics to probe the initial decomposition mechanisms of nitromethane. By comparing the impact on (010) surfaces and without impact (only heating) for nitromethane simulations, we found that proton dissociation is the first step of the pyrolysis of nitromethane, and the C–N bond decomposes in the same time scale as in impact simulations, but in the nonimpact simulation, C–N bond dissociation takes place at a later time. At the end of these simulations, a large number of clusters are formed. By analyzing the trajectories, we discussed the role of the hydrogen bond in the initial process of nitromethane decompositions, the intermediates observed in the early time of the simulations, and the formation of clusters that consisted of C–N–C–N chain/ring structures.
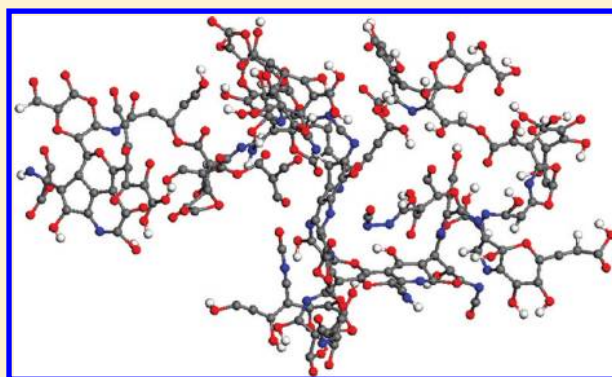
1. INTRODUCTION

Nitromethane (CH_3NO_2 or NM) has attracted lots of attention because it is the prototypical explosive, and its study can help us understand the reaction mechanism or initiation mechanism of more complex energetic materials such as RDX and HMX. For this reason, lots of experiments,[1−6] calculations based on the first principle,[7−13] and classical molecular dynamics simulations[14−19] have been conducted on it. Among previous research, there exist two viewpoints about the first step in the decomposition process of nitromethane, namely proton dissociation or C–N bond scission. The C–N bond, which has the lowest dissociation energy in gas phase NM,[20] is always thought as the first to decompose. However, more recent studies based on the first principle support the viewpoints that the proton decomposition is prior to C–N bond scission. Margetis et al.[13] found that under uniaxial compression the C–H bond highly stretched and leads to proton dissociation. By comparing the decompositions of NM under normal and high pressure, Xu and co-workers[8] found the early reactions are proton redistribution and C–N bond dissociation. And long chain structures are found in their final products, which is in agreement with the recent work carried out by Chang et al.[7] Citroni and co-workers[21] also proposed a proton redistribution decomposition pathway of NM at high static pressure through the formation of $CH_2NO_2^-$ and CH_3NOOH^+. Chang et al. reported a pathway $CH_3NO_2 \rightarrow CH_2HONO \rightarrow CH_3O + NO$ (where CH_2HONO represents a four-membered ring structure[7]) of NM decomposition via a Car–Parrinello molecular

dynamics study, and noteworthy, they found long carbon chain structures that consisted of pure CN fragments in their final products. Han et al.[22] carried out a high density and high temperature research of solid NM, and they found the first event in reactions are the proton transfer, leading to the formation of CH_2NO_2 and CH_3NOOH at $T = 3000$ K, and reaction $CH_3NO_2 \rightarrow CH_3ONO$ at temperature 2000 and 2500 K. They further tested the accuracy of the ReaxFF under extreme conditions. First principle studies can give more accurate predictions of reactions; however, they are limited to several NM molecules due to the consumption of huge computation times. Meanwhile, the reactive force field,[23] which is based on quantum calculations, can describe the reaction with appropriate precision for larger systems, an approach closer to real systems. With these points in mind, we employed ReaxFF to probe the kinetic mechanism of the NM decomposition.

In previous study,[24] we discussed the formation of hydrogen bond in crystal nitromethane under high pressure, and in this work we choose the recently developed reactive force field (ReaxFF)[23,25] to further study the decomposition process of the solid NM block that contains nearly 2000 atoms under different conditions. By comparing the different MD simulations, we offer research of the decomposition process

of nitromethane with respect to statistics and mainly discuss the initial decomposition mechanism, intermediate of reactions, and the formation of clusters in the final product.

2. SIMULATION DETAIL

We employ the reactive force field (ReaxFF),[23,25] which is included in *LAMMPS* package,[26] and use parameters developed for nitramines (ReaxFF$_{nitro}$)[25,27] to simulate the decomposition process of solid NM. ReaxFF is a potential based on quantum mechanics that can simulate chemical reactions of materials. It uses a general relationship between bond distance and bond order, which determines bond energy, and can give a proper description of the dissociation and formation of bonds between atoms.

The structure of crystalline nitromethane belongs to the orthorhombic space group $P2_12_12_1$ having $Z \cong 4$ molecules in the unit cell with lattice parameters $a = 5.228$ Å, $b = 6.293$ Å, $c = 8.664$ Å, $\alpha = \beta = \gamma = 90°$ (Figure 1) known from X-ray
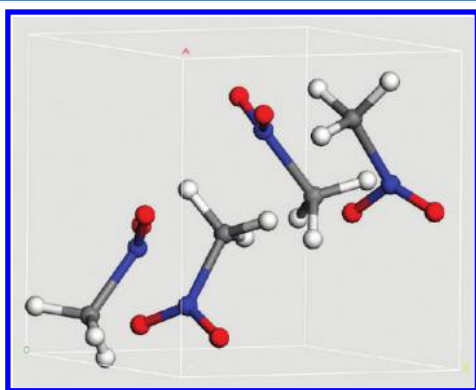
Figure 1. Unit cell of nitromethane crystal. Crystal lattice parameters are detected at $T = 213-216$ K and ambient pressure: $a = 5.228$ Å, $b = 6.293$ Å, $c = 8.664$ Å, $\alpha = \beta = \gamma = 90°$, and orthorhombic space group $P2_12_12_1$.

single crystal data.[6] The coordinate for these simulation are collected and minimized (relaxing atomic positions and lattice parameters) at low temperature (300 K, 0.3 GPa) with ReaxFF MD.

Three independent MD simulations have been conducted totally. (I) One simulation box contains two identical blocks measuring $18.394 \times 22.101 \times 15.152$ Å³ with 896 atoms (Figure 2a) applied with two-dimensional periodic conditions (i.e., $4a \times 2c$, and 52.00 Å in the b direction), creating two-dimensional periodic interfaces for interactions between double (010) surfaces. In the b direction, an open boundary can avoid collision between the reflected block and the repeated block, but the rapid decrease of the pressure of the system causes the block to rapidly turn into the gaseous state; therefore, open boundary conditions are hard for reactions. This in fact results in shock wave propagation in the b direction, but we did not consider this effect in detail for simplicity. It is widely accepted that surfaces are the places that have hot spots where chemical reactions occur more easily, because molecules in the surface are loosened and have more freedom. We use the *NVE* ensemble to simulate the impact of two NM blocks on (010) surfaces in this simulation, and the two blocks have velocities of +3 and −3 km/s, respectively. (II) The same box and velocities of two slabs as (I) but with the *NVT* ensemble are employed with a Berendsen thermostat[28] of 2500 K for a comparison. (III) The
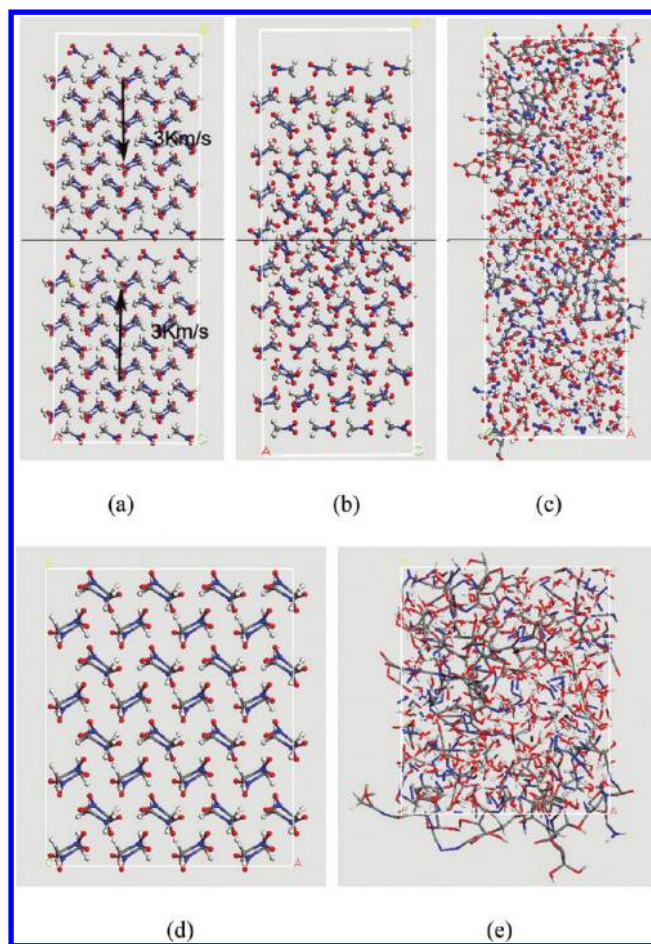
Figure 2. (a) Crystal structure of NM. We assign velocities of +3 and −3 km/s, respectively, to these two NM blocks and make it impact on the (010) surface. (b) Several femtoseconds after collision. (c) Snapshot of simulation box after simulation time of 60 ps. (d) Simulation of single crystal nitromethane block, a supercell of $4a \times 4b \times 4c$, measuring $18.394 \times 22.101 \times 30.304$ Å³. (e) Snapshot of the single crystal nitromethane without collision after a simulation time of 50 ps. Red represents O, white H, gray C, and blue N, respectively.

last simulation box contains one crystal NM block with three-dimensional periodic conditions measuring $18.394 \times 22.101 \times 30.304$ Å³ ($4a \times 4b \times 4c$) and having 1792 atoms with a density of 2.106 g/cm³, and *the NVT* ensemble is employed with a Berendsen thermostat of 2500 K.

We heat the reaction system step by step to give the system a low heating rate.[19,29] All the simulations use a time step of 0.1 fs to allow ReaxFF to describe reactions correctly at high temperature.[30] The total simulation times of all the above are about 0.1 ns. We use a *neigh_modify* key word of *every 1 delay 0 check no* in *LAMMPS* to build the atom neighbor list for every MD step; therefore, this allows ReaxFF to compute the bond order in each MD step. In the first simulation, the MD run is interrupted after about 10 ps due to continuous exothermic reactions, and we restart the simulation with the *NVT* ensemble with a Berendsen thermostat of 2500 K to cool the reaction system down to inspect the final products.

3. RESULTS AND DISCUSSION

To test the accuracy of the ReaxFF potential, we calculate lattice parameters of crystal NM at room temperature and under pressures 7.6, 11.0, and 15 GPa and at temperatures of

78, 228, and 293 K under zero pressure (Table 1). The total length of these test runs is 2.0 ps, and lattice parameters are

Table 1. Comparation of Lattice Parameters between ReaxFF MD and Experiments (Unit: Å)

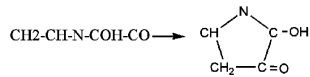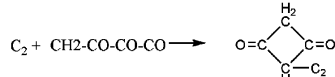|		a	b	c
11.0 GPa, 300 K	Citroni et al.[a]	4.607	5.636	7.771
	ReaxFF	4.608	5.537	7.592
15.0 GPa, 300 K	Citroni et al.[a]	4.540	5.534	7.687
	ReaxFF	4.531	5.444	7.465
0 GPa, 228 K	Cromer et al.[b]	5.244	6.320	8.730
	ReaxFF	5.223	6.275	8.604
0 GPa, 293 K	Cromer et al.[b]	5.270	6.375	8.832
	ReaxFF	5.231	6.284	8.617
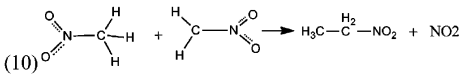
[a]Reference 2. [b]Reference 5.

averaged after equilibrium. Parameters computed by ReaxFF MD are in good agreement with experimental data.
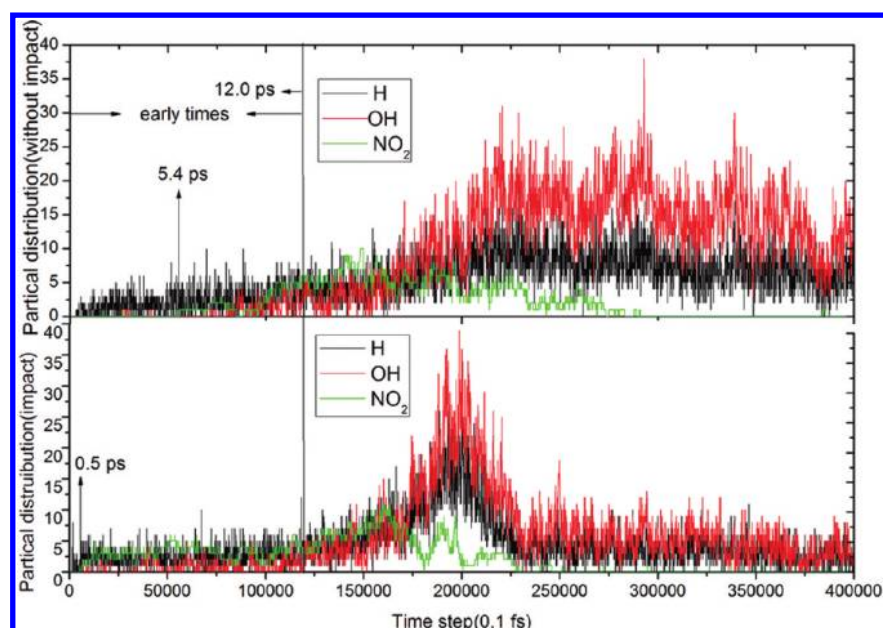
We use VMD[31] and our *FINDMOLE* tool to visualize and analyze the MD trajectories. In earlier times in our simulations, we observed three reactions in early steps of the NM decomposition: (I) Well-known proton transfer.[10,11,13,21,22] Rupture of the C—H bond started at 0.4–0.5 ps under a temperature of 2500 K in three simulations; this was in quantitative agreement with the CASTEP simulation of hot and dense NM reported by Manaa et al.[11] (0.785 ps), and ReaxFF simulations (0.05, 0.1, 0.3 ps) carried out by Han and collaborators.[22]

Protons react with the NO$_2$ and CH$_3$NO$_2$ forming OH radicals, most of OH radical forming H$_2$O and alcohols gradually. OH radicals and H$_2$O have an important role in the further decomposition of NM molecules. They not only supply oxidized reactants of reactions but also act as catalysts helping the C—N and N—O bond dissociations. The dissociated protons have an average charge of about 0.341, the OH radicals have an average charge about −0.242, and HO$_2$ is about −0.360 in units of $q_e = 1.602 \times 10^{-19}$, indicating under condensed fluid phase conditions the reaction is not ideally ionic. (II) C—N bond scission (reactions 1, 5, 10, and 11, in Table 2 observed in collision simulations) started at 0.4–0.5 ps in the first and the second simulations, and at 5.3–5.4 ps in the third simulation. Due to shearing[32] induced by the impact, C—N bonds, which are nearly perpendicular to the shearing direction (b direction), have a stronger vibrational motion and, therefore, can break up more easily. A few split C—N bonds can be observed in *NVE* and *NVT* simulations of two-block impact, and in nonimpact *NVT* simulation the C—N bond scission is observed at a later simulation time. This is consistent with the research reported by Chang et al. Reaction 11 in Table 2 is also reported by their collision simulation, and Zhu[33] also discussed a pathway of decompositions: CH$_3$NO$_2$ → CH$_3$ONO → CH$_3$O + NO. (III) The N—O bond dissociation and proton dissociations result in the forming of CN radicals and NO molecules. The CN radicals are the main reactants in the forming of ···C—N—C—N··· chains/ring structures as in Chang's simulations.[7] Reactions are shown by reactions 12–15, 23, and 24 in Table 2.

Table 2. Intermediate Products and Reactions Observed in All Reactive MD Simulations: Two-Block Collision at Double (010) Surface and Perfect Crystal Decomposition

Figure 3. Comparison of the evolution of particle numbers at early simulation times between simulations with and without impact.

The hydrogen ejection causes the methyl group in the NM molecule to have unpaired electrons that are free for reactions. The incoming CN fragment, which also has unpaired electrons, will reconnect with CH_2NO_2, which has unpaired electrons, forming stable structures of $C-N-CH_2-NO_2$, the nitro end of the structure subsequently undergoes several reactions, resulting in the structure of $C-N-C-N$, and step by step, more and more methyl group and CN fragments connected with each other forming $\cdots C-N-C-N \cdots$ long chain/ring structures.

3.1. Evolution of Particle Numbers as a Function of Simulation Time. We analyzed the evolution of particle numbers as a function of time (Figures 3 and 4). The simulation box contains 256 molecules, 1792 atoms totally, including 768 H, 256 C, 256 N, and 512 O atoms, respectively. The number of protons becomes nonzero in each simulation at about 0.5 ps, which is when decompositions start, and has a peak distribution at about 20.1 ps. H_2O is the main product in the three simulations, the number of H_2O at the end of all simulations is approximately 300. In all simulations, H_2O can act as a catalyst in a lot of reactions such as N−O, C−N, N−O, C−H, and C−O bond dissociation and reactions 13, 16, 18, and 21 listed in Table 2. The number of NO_2 is nonzero at about 0.5 ps in *NVE* and *NVT* simulations of impacts, about the same time period as when the number of protons becomes nonzero in all simulations. However, in *NVT* simulation of a single NM block (Figure 3), the starting time when the number of NO_2 becomes nonzero is 5.4 ps, a much later time compared with 0.5 ps of the two-NM collision simulation. It shows that proton redistributions and C−N bond scission are the early events in collision-induced decompositions, yet in one NM block without impact, C−N dissociation is not the first step, because the rupture of the C−N bond is not observed *early* in the simulation. NO_2 and NO exist in all simulations, but at the end of each simulation (after a simulation time of about 0.1 ns), there are only a few NO_2 and NO, because NO_2 and NO will further react with other radicals, generating larger molecular structures such as rings and chains (reactions 6 and 7 in Table 2
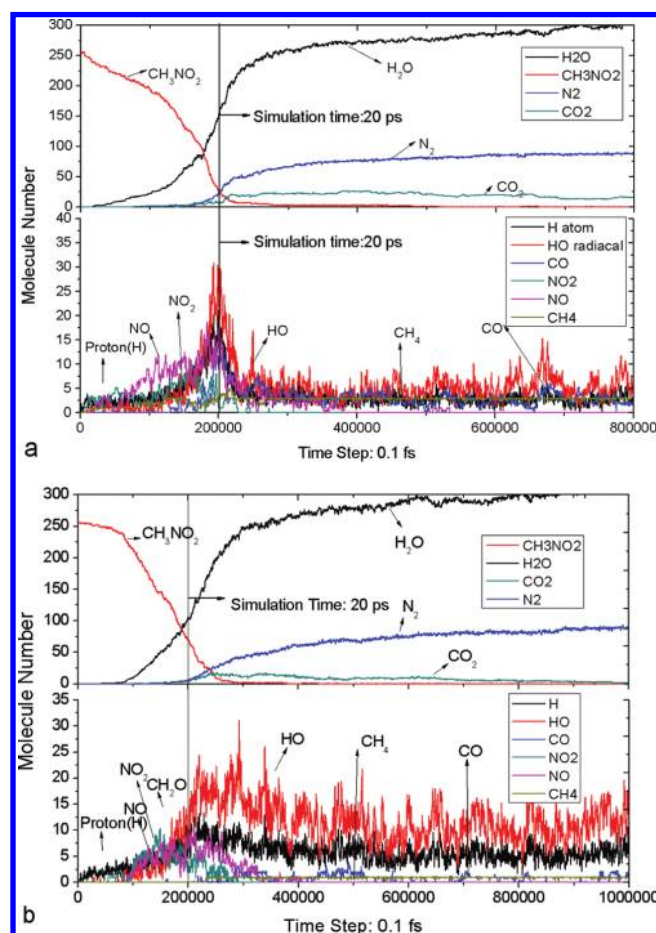
Figure 4. Molecule number distribution as a function of MD time step (0.1 fs). Total simulation times are 80 and 100 ps, respectively. (a) Distributions of the simulation of two NM blocks colliding at the double (010) surface with the *NVT* ensemble (*T* = 2500 K). The average pressure of this simulation is 11.56 GPa. (b) Distribution of the particle number of a single NM block with the *NVT* ensemble (*T* = 2500 K). The average pressure of this simulation is 19.74 GPa.

and Figure 6). CO also has a large number in the decomposition process, but after a peak distribution at about 30 ps in all simulations (Figure 4a,b), the number of CO has decreased, as it will react with other C−N structures forming ⋯C−N−C−O⋯ chain/ring structures.

Figure 4 showed the evolution of the number of molecular fragments in the *NVE* simulation of two NM collisions and *NVT* simulations of a single NM block. *NVT* simulations of the two NM collisions have a particle distribution similar to that of the *NVE* simulations. Between 15.5 and 25.0 ps the number of NM steeply declines, the number of N_2, H_2O, and CO_2 rapidly rises, and the number of NO_2, proton, NO, NO_2, and radical OH have a peak distribution; these shed light on the conclusion that decompositions mainly take place at this time scale. After this time scale, i.e., after a simulation time of about 25 ps, these structures reach a dynamic equilibrium with C−N, O−C−O, N−O, C−H, and O−N−N−O bond dissociation and recombination: O + H → OH, OH + H → H_2O, and radicals CO, CN, NO, OH, NH, and $CH_{n(n<4)}$ groups that have unpaired electrons linked with each other, forming chains/rings.

3.2. Role of Hydrogen Redistributions in NM Decompositions. From the start of simulation to the time when molecule (or radical) numbers are rapidly increasing or decreasing, several reactions have been observed, such as proton transfer, OH radical formation, and C−N bond scission; they are important for the decomposition mechanism study of NM, because in this interval, new reactants are prepared for further reactions. We call this time period the "early time" (0−12.0 ps) in the simulations. The intermolecular hydrogen bond has an important role in both C−H and N−O bond dissociation in the early time of the simulation. Intermolecular O−H bond distance in (1) is 1.79 Å,

$$\text{(1)}$$
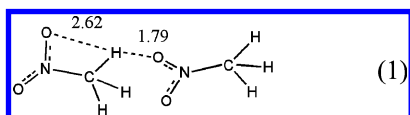
and the innermolecular O⋯H distance is 2.62 Å. The attractions from neighboring O atoms cause the proton transfer to it, forming $CH_2(OH)NO_2$, and CH_3NO. This is consistent with the work reported by Han et al.[22] The time they listed for the breaking and forming of the C−H and O−H bond in all simulations indicates that the breaking of the C−H bond is always under the attraction of oxygen in nearby molecules. The transferred hydrogen atoms will attach on a neighboring O atom, and some of them will further cause the N−O bond dissociation, generating C−N groups and OH radicals.

$$\text{(2)}$$
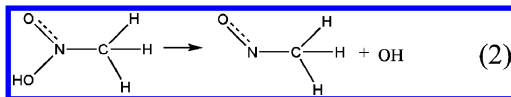
The generated OH radical can be helpful in the scissions of C−N and N−O bonds; for example, the OH radical can bond with neighboring O atoms, and the proton transfers between two oxygens, generating a free O atom. It will react with neighboring NM molecules in the following way

$$\text{(3)}$$
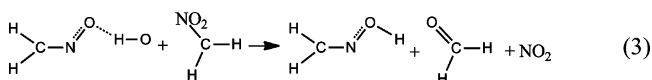
and generate stable CH_2O and NO_2 molecules. Citroni[21] also observed a similar H atom or H^+ ion migration process between neighboring NM molecules: $2CH_3NO_2 \rightarrow CH_3NOOH +$

CH_2NO_2, and the O atom in CH_3NOOH was attracted by the nearby N atom, forming new N−O bond, i.e., structure $H_2C\text{-}N\text{-}O\text{-}N\text{-}CH_3$.
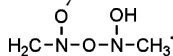
3.3. Intermediates Observed in Simulations. Parts of intermediates (INT for short) that have a lifetime about 0.3−0.5 ps in the simulations are listed in Figure 5. Through these
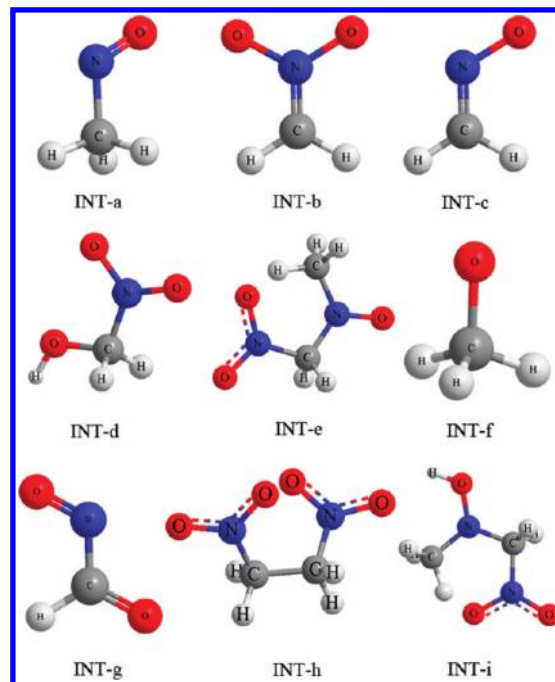

Figure 5. Intermediates observed in the early simulation time (0−12 ps).

structures we can study the pathways of the decomposition process of solid state NM. These structures are observed in the time period of about 0−12 ps (early time in the simulations).

In Figure 5, INT-a, INT-b, and INT-c are formed by proton distributions and N−O bond decompositions. There are a large number of these three structures in simulations. INT-a and INT-b are also reported by Gutsev et al.[34] in the investigation of the decomposition energies through different decay channels of methylnitrite (CH_3ONO). INT-d is formed when the OH radical reacts with CH_2NO_2, and it later undergoes a C−N bond cleavage forming NO_2 and formaldehyde molecules.

$$OH + CH_2NO_2 \rightarrow CH_2(OH)NO_2 \tag{4}$$

$$CH_2OH \rightarrow CH_2O + H \tag{5}$$

CH_2NO_2 reacts with CH_3NO forming INT-e and undergoes N−O bond decompositions forming the C−N−C−N chain. CH_3O(INT-f) is formed by reaction 6 in our simulations,

$$\text{(6)}$$
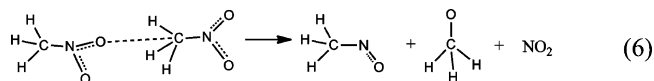
one NM molecule collides with another, causing the NO_2 group dissociation, forming products CH_3NO, CH_3O, and NO_2. C−H bond decomposes in INT-f, forming a formaldehyde molecule, which is consistent with Martínez-Núñez's study;[35] they computed the reaction rate constants for CH_3O + NO → CH_3ONO with classical trajectory and canonical variational

transition state theory (CVTST). They conclude that reactions 7−9 are decomposition channels for CH_3O.

$$CH_3O + NO \leftrightarrow CH_3ONO \qquad (7)$$

$$CH_3ONO \rightarrow CH_2O + HNO \qquad (8)$$

$$CH_3O \rightarrow CH_2O + H \qquad (9)$$

Reaction channel 8 is also reported by Zhu[33] and Chang.[7] INT-g undergoes a C−N bond cleavage (reaction 10) forming HCO and NO.

$$\text{(structure)} \longrightarrow HCO + NO \qquad (10)$$
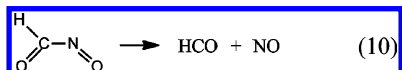
INT-h undergoes a C−N bond dissociation forming NO_2 and $CH_2CH_2NO_2$ structures. The C−N bond and N−O bond dissociate in INT-i forming NO_2, OH, and C−N−C.

$$\text{(structure)} \longrightarrow OH + NO_2 + H_3C\text{-}N\text{-}CH_2 \qquad (11)$$
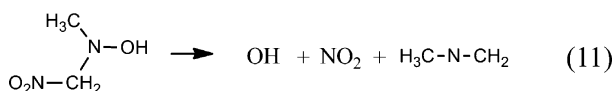
INT-d, INT-h, INT-g, INT-i, and reactions 2, 4, and 8−11 in Table 2 are pathways of C−N bond decompositions observed in our simulations.

Parts of these intermediates are partially ionized in the dense fluid phase, as their charges are not equal to zero. INT-c has a charge of about 0.09, INT-d has a charge of about −0.24, INT-f has a charge of about 0.41, and INT-g has a charge of about −0.27. INT-a, INT-b, INT-c, INT-h, and INT-i are electrical neutrality. More intermediates and charge distributions are available in the Supporting Information.

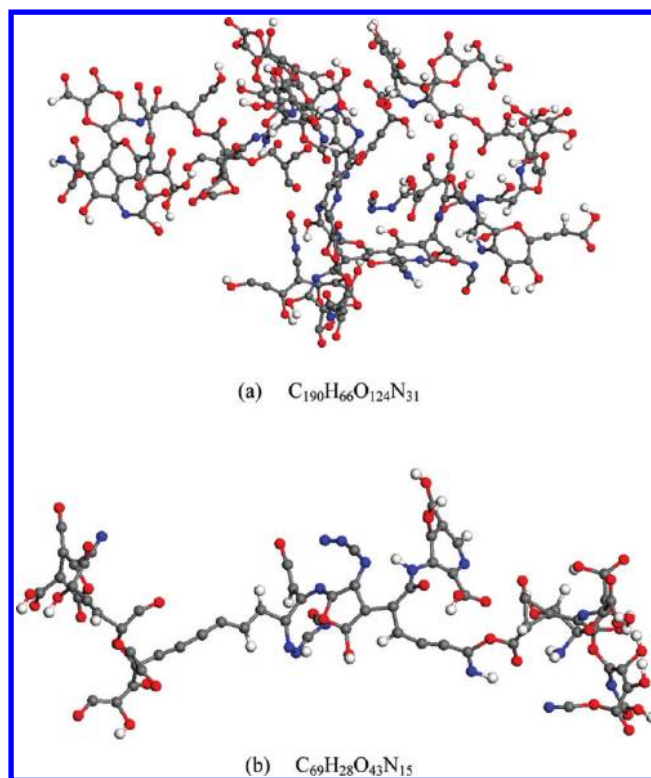### 3.4. Clusters Structures Formed in MD Simulations.

Compared with the final products from Chang's[7] computation, not only long C−N−C−N chain structures are observed in our simulation but also ring structures (Figures 6 and 7). Larger C
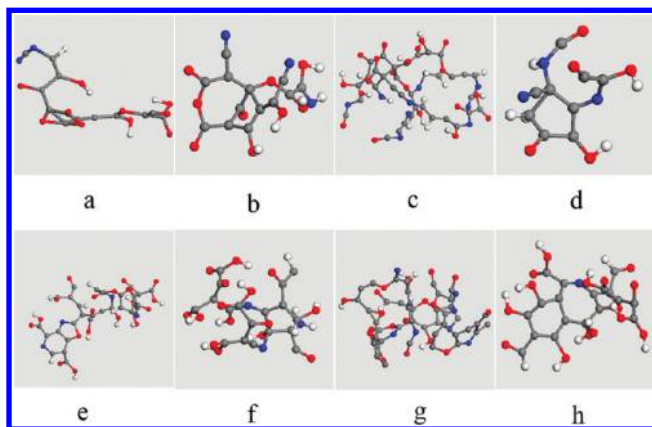
Figure 6. Small clusters formed during reactive MD simulations. C atoms are in gray, O is in red, H is in white, and N is in blue.

clusters are formed by the rich N and O carbon molecular fragment (shown in the Figure 2 of Supporting Information) step and step; these fragments are much the same with what Citroni[21] have reported (in their Supporting Information), both rich in N and O. CH_2O (formaldehyde), CO_2, CH_3NO (nitrosomethane), and CH_2OHNO_2 (nitromethanol) in their Supporting Information are also observed in our simulations.

C clusters are also found in thermal decomposition of 1,3,5-tiamino-2,4,6-trinitrobenzene (TATB) and octahydro-1,3,5,7-tetranitro-1,3,5,7-tetrazocine (HMX).[27] In our simulation, the

Figure 7. Larger C clusters formed during ReaxFF simulation. (a) $C_{190}H_{67}O_{124}N_{33}$, the largest cluster formed in the simulation. (b) $C_{69}H_{28}O_{43}N_{15}$.

chain and ring structures are formed by the connection of molecular fragments as shown by reactions 22 and 24 in Table 2.

4. CONCLUSIONS

We studied the decomposition of NM by comparing the decomposition induced by the impact of two NM blocks on two (010) surfaces and thermal decomposition of a single NM block applying ReaxFF MD simulations with a total simulation time about 100 ps. Through simulations, we offered a reaction process study in perspective of statistics.

In the early time of the simulation: (1) C−H dissociation is the first step in all simulations. (2) C−N and C−H bond scissions take place almost at the same time in the early steps of NVE and NVT simulations of two collided NM blocks, because the collision makes the weaker bonds, such as C−N and N−O, break up more easily, whereas the C−N bond breaking takes place at a later time in NVT simulations of a single NM block. (3) The −NO/−NO_2 group reacts with the H atom, generating OH and CN or other fragments; this reaction takes place in all simulations.

Hydrogen bonding offered pathways for H atom translocations, such as C−H···O or O···H···O, the proton transferred from one ion to other, and further generating an OH radical, which has an important role in other bond dissociations, such as N−O and C−N bonds.

CN, CO, and NO groups are reactants for chain/ring structures. Radicals such as CN, NO, CO, OH, and CC groups that have unpaired electrons connected with each other, and step by step, forming chain/ring structures and larger clusters.

■ ASSOCIATED CONTENT

Ⓢ Supporting Information

Molecular fragments observed in the early time and chain structures observed in other time scales. This information is available free of charge via the Internet at http://pubs.acs.org.

■ AUTHOR INFORMATION

Corresponding Author
*E-mail: hongzhang@scu.edu.cn.

Notes
The authors declare no competing financial interest.

■ ACKNOWLEDGMENTS

■ REFERENCES

(1) Ouillon, R.; Pinan-Lucarre, J. P.; Canny, B.; Pruzan, P.; Ranson, P. *J. Raman Spectrosc.* **2008**, *39*, 354−362.

(2) Citroni, M.; Datchi, F.; Bini, R.; Vaira, M. D.; Pruzan, P. *J. Phys. Chem. B* **2008**, *112*, 1095−1103.

(3) Zhang, Y.-X.; Bauer, S. H. *J. Phys. Chem. B* **1997**, *101*, 8717−8726.

(4) Courtecuisse, S.; Cansell, F.; Fabre, D.; Petitet, J.-P. *J. Chem. Phys.* **1995**, *102*, 968−974.

(5) Cromer, D. T.; Ryan, R. R.; Schiferl, D. *J. Phys. Chem.* **1985**, *89*, 2315−2318.

(6) Bagryanskaya, Y.; Gatilov, Y. V. *J. Struct. Chem.* **1976**, *24*, 150−151.

(7) Chang, J.; Lian, P.; Wei, D. Q.; Chen, X. R.; Zhang, Q. M.; Gong, Z. Z. *Phys. Rev. L* **2010**, *105*, 188302.

(8) Xu, J. C.; Zhao, J. J. *Chin. Phys. Soc.* **2009**, *58*, 4144−4149.

(9) Conroy, M. W.; Oleynik, I. I.; Zybin, S. V.; White, C. T. *J. Phys. Chem. A* **2009**, *113*, 3610−3614.

(10) Liu, H.; Zhao, J. J.; Wei, D. Q.; Gong, Z. Z. *J. Chem. Phys.* **2006**, *124*, 124501.

(11) Manaa, M. R.; Reed, E. J.; Fried, L. E.; Galli, G.; Gygi, F. *J. Chem. Phys.* **2004**, *120*, 10146−10153.

(12) Fried, L. E.; Reed, E. J.; Manaa, M. R. *Shock Compression of Condensed Matter* **2003**, *706*, 327−330.

(13) Margetis, D.; Kaxiras, E. *J. Chem. Phys.* **2002**, *117*, 788−799.

(14) Siavosh-Haghighi, A.; Sewell, T. D.; Thompson, D. L. *J. Chem. Phys.* **2010**, *133*, 194501.

(15) Siavosh-Haghighi, A.; Dawes, R.; Sewell, T. D.; Thompson, D. L. *J. Phys. Chem. B* **2010**, *114*, 17177−17186.

(16) Siavosh-Haghighi, A.; Richard, D.; Sewell, T. D.; Thompson, D. L. *J. Chem. Phys.* **2009**, *131*, 064503.

(17) Siavosh-Haghighi, A.; Thompson, D. L. *J. Chem. Phys.* **2006**, *125*, 184711.

(18) Sorescu, D. C.; Rice, B. M.; Thompson, D. L. *J. Phys. Chem. B* **2000**, *104*, 8406−8419.

(19) Zheng, L. Q.; Luo, S. N.; Thompson, D. L. *J. Chem. Phys.* **2006**, *124*, 154504.

(20) Pedley, J. B.; Naylor, R. D.; Kirby, S. P. *Thermochemical Data of Organic Compounds*, 2nd ed.; Chapman: New York, 1986.

(21) Citroni, M.; Bini, R.; Pagliai, M.; Cardini, G.; Schettino, V. *J. Phys. Chem. B* **2010**, *114*, 9420−9428.

(22) Han, S. P.; van Duin, A. C. T.; Goddard, W. A.; Strachan, A. *J. Phys. Chem. B* **2011**, *115*, 6534−6540.

(23) van Duin, A. C. T.; Dasgupta, S.; Lorant, F.; Goddard, W. A. *J. Phys. Chem. A* **2001**, *105*, 9396−9409.

(24) Guo, F.; Cheng, X. L.; Zhang, H. *J. Theor. Comput. Chem.* **2009**, *9*, 315−325.

(25) Strachan, A.; van Duin, A. C. T.; Chakraborty, D.; Dasgupta, S.; Goddard, W. A. *Phys. Rev. L* **2003**, *91*, 098301.

(26) Plimpton, S. *J. Comput. Phys.* **1995**, *117*, 1−19.

(27) Zhang, L.; Zybin, S. V.; van Duin, A. C. T.; Dasgupta, S.; Goddard, W. A. *J. Phys. Chem. A* **2009**, *113*, 10619−10640.

(28) Berendsen, H. J. C.; Postma, J. P. M; Gunsteren, W. F. v.; DiNola, A.; Haak, J. R. *J. Chem. Phys.* **1984**, *81*, 3684−3690.

(29) Bai, X. M.; Li, M. *Phys. Rev. B* **2008**, *77*, 134109.

(30) Chenoweth, K.; van Duin, A. C. T.; Goddard, W. A. *Phys. Chem. A* **2008**, *112*, 1040−1053.

(31) Humphrey, W.; Dalke, A.; Schulten, K. *J. Mol. Graph.* **1996**, *14*, 33−38.

(32) Arman, B.; An, Q.; Luo, S. N.; Desai, T. G.; Tonks, D. L.; Çağin, T.; Goddard, W. A. *J. Appl. Phys.* **2011**, *109*, 013503.

(33) Zhu, R. S.; Lin, M. C. *Chem. Phys. Lett.* **2009**, *478*, 11−16.

(34) Gutsev, G. L.; Jena, P.; Bartlett, R. J. *J. Chem. Phys.* **1999**, *110*, 403−411.

(35) Martínez-Núñez, E.; Borges, I.; Vázquez, S. A. *J. Phys. Org. Chem.* **2001**, *15*, 123−129.